Environ Monit Assess (2020) 192:733
https://doi.org/10.1007/s10661-020-08688-2

Integrated GIS-based RUSLE approach for quantification of potential soil erosion under future climate change scenarios

Madhusmita Behera · Dipaka R. Sena · Uday Mandal · Pradeep S. Kashyap · Sonam S. Dash

Received: 23 June 2020 / Accepted: 15 October 2020

Abstract Human-induced agricultural and developmental activities cause substantial alteration to the natural geography of a landscape; thereby accelerates the geologic soil erosion process. This necessitates quantification of catchment-scale soil erosion under both retrospective and future scenarios for efficient conservation of soil resources. Here, we present a revised universal soil loss equation (RUSLE) based soil erosion estimation framework at an unprecedentedly high spatial resolution (30 × 30 m) to quantify the average annual soil loss and sediment yield from an agriculture-dominated river basin. The input parameters were derived by using the observed rainfall data, soil characteristics (soil texture, hydraulic conductivity, organic matter content), and topographic characteristics (slope length and percent slope) derived from digital elevation model (DEM) and satellite imageries. The developed approach was evaluated in the Brahmani River basin (BRB) of eastern India, wherein the different RUSLE inputs, viz., rainfall erosivity (*R* factor), soil erodibility (*K* factor), topographic (*LS* factor), crop cover (*C* factor), and management practice (*P* factor) factors have the magnitude of 1937 to 4867 MJ mm ha^{-1} h^{-1} $year^{-1}$, 0.023 to 0.039 t h ha MJ^{-1} ha^{-1} mm^{-1}, 0.03 to 74, 0.16 to 1, and 0 to 1, respectively. The estimated average annual soil loss over the BRB ranged from 0 to 319.55 t ha^{-1} $year^{-1}$, and subsequent erosion categorization revealed that 54.2% of basin area comes under extreme soil erosion zones in the baseline period. Similarly, the sediment yield estimates varied in the range of 0.96 to 133.31 t ha^{-1} $year^{-1}$, and 35.81% area were identified as high soil erosion potential zones. The extent of erosion under climate change scenario was assessed using the outputs of HadGEM2-ES climate model for the future time scales of 2030, 2050, 2070, and 2080 under the four representative concentration pathways (RCPs) 2.6, 4.5, 6.0, and 8.5. The severity of soil erosion under climate change is expected to have a mixed impact in the range of −25 to 25% than the baseline scenario. The outcomes of this study will serve as a valuable tool for decision-makers while implementing management policies over the BRB, and can be well extended to any global catchment-scale applications.

M. Behera
Odisha, India

D. R. Sena · U. Mandal (✉)
Hydrology and Engineering Division, ICAR-Indian Institute of Soil and Water Conservation, Dehradun 248195, India
e-mail: uget.uday.mandal@gmail.com

D. R. Sena
e-mail: drsena_icar@yahoo.co.in

P. S. Kashyap
Department of Soil and Water Conservation Engineering, G. B. Pant University of Agriculture and Technology, PantNagar, Uttarakhand 263145, India
e-mail: pskashyap@gmail.com

S. S. Dash (✉)
School of Water Resources, IIT Kharagpur, Kharagpur, West Bengal 721302, India
e-mail: ssdash@yahoo.com

Published online: 29 October 2020

Keywords Climate change · HadGEM2-ES · RCP · RUSLE · Sediment yield · Soil erosion

Abbreviations

ArcGIS	Aeronautical Reconnaissance Coverage Geographic Information System
ASTER	Advanced spaceborne thermal emission and reflection radiometer
BMPs	Best management practices
BRB	Brahmani River basin
C-factor	Crop cover factor
DEM	Digital elevation model
e.g.	Exempli gratia
et al.	And others
GCM	General circulation model
GIS	Geographical information system
HadGEM2-ES	Hadley Center Global Environmental Model, version 2 (Earth System)
i.e.	that is
ICAR	Indian Council of Agricultural Research
IDW	Inverse distance weighting
IISWC	Indian Institute of Soil and Water Conservation
IMD	India Meteorological Department
IPCC	Intergovernmental panel on climate change
K-factor	Soil erodibility factor
LS-factor	Topographic factor
LULC	Land use land cover
MSL	Mean sea level
MUSLE	Modified universal soil loss equation
NBSS&LUP	National Bureau of Soil Survey and Land Use Planning
NDVI	Normalized difference vegetation index
NICRA	National innovations on climate resilient agriculture
NRSC	National remote sensing Centre
OLI	Operational land imager
P factor	Management practice factor
RCM	Regional climate model
RCPs	Representative concentration pathways
R factor	Rainfall erosivity factor
RUSLE	Revised universal soil loss equation
SCS	Soil conservation service
SDR	Sediment delivery ratio
TM	Thematic mapper
USA	United States of America
USDA	United States Department of Agriculture
USGS	United States Geological Survey
USLE	Universal soil loss equation
viz	Namely

Introduction

Soil erosion is an adverse hydro-geologic phenomena consisting of detachment and transportation of surface soil particles from its initial location to the nearby location for subsequent accumulation. Water plays the key role in the detachment, transportation, and deposition phase of soil erosion processes. The soil erosion process gets accelerated by considerable human activities across many places of the globe (Gabriels and Cornelis 2009). Moreover, poor land-use practices also lead to considerable increase in the soil erosion (Arnáez et al. 2015).

Globally, a number of soil loss assessment models have been developed by several researchers, but each model has its inherent limitations based on the input availability, scale of application, and involved degree of complexity (Chandramohan et al. 2015). Hence, no single soil loss prediction model can dispense any solid outcomes for assessing the soil erosion in a regional scale application. Many complex phenomena influencing the soil erosion process were hypothesized through simplified assumptions in order to smoothen the erosion modeling process. In the literature, a number of statistical/metric (empirical), conceptual (semi-empirical), and physical process-based (deterministic) models are existing; those quantify the soil erosion process is filed to regional-scale applications (Nearing et al. 2005). However, the global applications are mostly confined to the use of empirical models due to extensive data requirements and lack of expertise of the modeler. The empirical universal soil loss equation (USLE) (Wischmeier and Smith 1965) is the most conventional soil erosion model, developed based on extensive experimental data in the USA condition. The USLE model mainly accounts for the soil loss process in the form of sheet erosion followed by rill erosion occurred over an agricultural watershed. Upon gradual advancement in the soil erosion modeling, the modified universal soil loss equation (*MUSLE*) proposed by Williams and Berndt (1977) addressed the underlying limitations involved in USLE, i.e., non-accountability of gully erosion process and inability to compute the sediment deposition. For estimation of sediment yield, USLE

solely depends on the rainfall process but MUSLE predicts the same by incorporating the effect of runoff in the form of a peak runoff factor which is a consequence of antecedent moisture condition in a locality. Further, the revised universal soil loss equation (RUSLE) is extensively adopted for soil erosion risk assessment because of its flexibility in field-scale applications and serves as a conventional tool for conservational policy implementation (Kouli et al. 2009; Chen et al. 2011; Rawat et al. 2016; Mahala 2018).

The RUSLE estimates the average annual soil erosion over land surface by simple multiplication approach of several input factors, viz., rainfall erosivity factor (*R*), soil erodibility factor (*K*), slope length and steepness, combinely known as topographic factor (*LS*), cover management factor (*C*), and conservation practice factor (*P*) (Renard et al. 1997). Further, from the management perspective, the sediment yield has more practical implications than the potential soil erosion in a locality. In past studies, the sediment yield was estimated for the catchment using USLE or RUSLE in conjunction with an empirical parameter called sediment delivery ratio (SDR) (Boomer et al. 2008; Alatorre et al. 2010). This factor determines the transferability of sediments from the hill slopes into the nearby streams responsible for the erosion process. The selected study region, i.e., Brahmani River basin is a highly industrialized basin, wherein extensive earthworks resulting in significant alteration to the natural soil regolith causing higher soil erosion. Moreover, the occurrence of frequent floods due to anthropogenic changes in the upstream of the Brahmani River induces profound soil detachment in the floodplain; thereby moderates both detachment and transport process of soil erosion. The climate of a region corresponds to the long-term ($\geq$ 30 years) average weather condition of a region. It accounts for acutely complex internal mechanisms associated with individual meteorological variables which are highly dynamic in nature. As defined by the intergovernmental panel on climate change (IPCC), the climate change points to an alternation in the existing climatic condition of a locality which can be detected (e.g., by some statistical means) by analyzing the change in the variability of individual climate variables that may persist for a prolonged period (IPCC 4th Assessment Report, Climate change 2007). Certainly, some of the associated factors of RUSLE model tend to alter its behavior in a climate change context; hence, a significant variation will be observed in the soil erosion magnitude in the future time scales. This leads to the potential failure of the proposed policy (in baseline scenario) in the future time scales, and subsequently, the future time scales of the concerned location may experience landslide and flood havocs with very high periodicity. Ignoring these adverse consequences, a few past studies have quantified the climate change impact over catchment-scale soil erosion process with a lot of simplified assumptions.

From this extensive review, the following research gaps have been identified: (i) lack of studies in combining the RUSLE and geographical information system (GIS) approach to estimate the soil erosion potential in catchment-scale applications, (ii) a spatially distributed SDR estimation approach has not been adopted in soil erosion hazard studies, (iii) the past soil erosion modeling studies were carried out at a coarse spatial resolution which may lead to erroneous modeling outcomes, and (iv) no past studies quantified the soil erosion hazard under a climatic change context. Considering the above bottlenecks, this study tries to address the following research questions: (i) Will the GIS-RUSLE based soil erosion estimation approach provide a true insight about the catchment-scale erosion process? (ii) How useful will be the finer-scale (30 m) erosion modeling while implementing the conservation practices in critical areas? (iii) Does the SDR-based erosion assessment approach has an edge over the conventional RUSLE technique? (iv) What kind of variability in the soil erosion process could be expected in a changing future climatic scenario? Keeping these research questions in mind, the specific objectives of this study are (i) to develop an integrated GIS-based RUSLE approach to quantify the existing soil erosion potential in the Brahmani River basin, (ii) to estimate the actual soil loss (sediment yield) by a spatially distributed SDR approach over the basin, (iii) assessing the climate change impact on the soil erosion process using suitable general circulation model (GCM) for multiple future time scales.

Materials and methods

Description of the study area

The Brahmani River is one of the major seasonal flowing river in the state of Odisha. The formation of

this river has occurred from the confluence of two rivers, viz., South Koel and Sankh, which is situated between latitude 20° 28′ and 23° 35′ N and longitude 83° 52′ to 87° 30′ E. The basin is comprised of 39,633.12 km^2 area (Fig. 1). The total basin is spatially distributed over the following three states, such as 22,516, 15,405, and 1347 km^2 in Odisha, Jharkhand, and Chhattisgarh, respectively. The Sankh River, which is a major contributing river, originates from the border of Jharkhand-Chhattisgarh which is very close to the Netarhat Plateau. The other contributing river, South Koel also begins from Jharkhand, at Lohardaga, on the other side of a watershed from where Damodar River originates. The basin elevation ranges from 1 to 1169 m with respect to mean sea level (MSL). Almost half of the basin area is confined under 100 m elevation. Agriculture (*kharif* and *rabi* crop) and deciduous forest are the major land use classes, which combinedly covered 70% area of the total basin.

The Brahmani River flows through a length of approximately 446 km; thereby affects a considerable portion of land area surrounding it. The Brahmani river basin (BRB) lying in a tropical region and climate is predominantly semi-arid. The temperature ranges between 4 to 47 °C over the BRB region. The average annual rainfall is about 1305 mm with erratic variation occurs between 969 and 1574 mm. The spatial distribution of soil types indicate that the study area is categorized under three major soil classes, i.e., yellow, gravelly red, and red soil; wherein the central part of state Odisha, is enriched with loam soil texture, and loam and laterite soil texture are observed in the downstream of the basin.

Database

The key inputs for RUSLE consists of the digital elevation model (DEM), soil hydraulic parameters (sand, silt, clay, and organic matter content), spatial land use/land cover information, and daily precipitation data. Five tiles of 30-m spatial resolution ASTER DEM were obtained from the USGS earth explorer website (http://earthexplorer.usgs.gov) which completely encompassed the study area for watershed delineation and extraction of stream network (Fig. 1). Monthly average rainfall values of all the sub-basins within the BRB were procured from the India Meteorological Department (IMD) for the period of 1951–2014 (Adhikary et al. 2019; Dash et al. 2019; Dash et al. 2020a). The essential soil information, including the percentage of soil texture, organic matter, and soil permeability, were procured from the National Bureau of Soil Survey and Land Use Planning (NBSS&LUP), Nagpur, Maharashtra. The DEM was also utilized for topographic characterization such as slope length and steepness of the basin. For the classification of land use, NRSC land use information (scale 1:250000) was adopted and 16 distinct land use classes were identified. The Landsat TM 8 (OLI) images of the year 2015 were procured and utilized for calculating normalized difference vegetation index (NDVI) later which was utilized for estimating the crop coverage factor (*C* factor).

Model structure

This study adopts RUSLE model to estimate the potential soil erosion in a tropical Indian River basin. It requires meaningful input variables and those could be easily got from the available data sources. Presently, RUSLE model is the best-known modeling tool to simulate the actual soil potential at coarse to fine spatial scales, i.e., from field scale to country scale or regional and to subsequent local scales. The model is also applicable to typical landform where extensive mining is carried out, and the soil is directly exposed to the impact of raindrops, and subsequently, affects crop lands, range lands, forest lands, construction sites, reclaimed lands, landfills, parks, military training sites causing rapid increase in surface runoff. As per Renard et al. (1997), the input parameters of RUSLE, which were estimated using the continuous information of weather, land use, soil, and topographical information, and subsequently, evaluates the streamflow dynamics and soil erosion caused due to direct correlation between rainfall and surface runoff process. This model has been extensively used for estimating the soil erosion potential and its risk assessment thereby provides guidelines to rehabilitate the erosion-prone areas through adoption of suitable management policy (Ostovari et al. 2017; Biswas and Pani 2015).

Parameterization of RUSLE model

RUSLE acts as a powerful model, which quantifies the long-term rill and inter-rill erosion process occurring over various agricultural and forest catchments. It is quite similar to the structure of USLE, but with a simplified nature in terms of the optimal use of the available data sources. RUSLE model uses five model parameters to estimate the average annual soil loss in a region. The

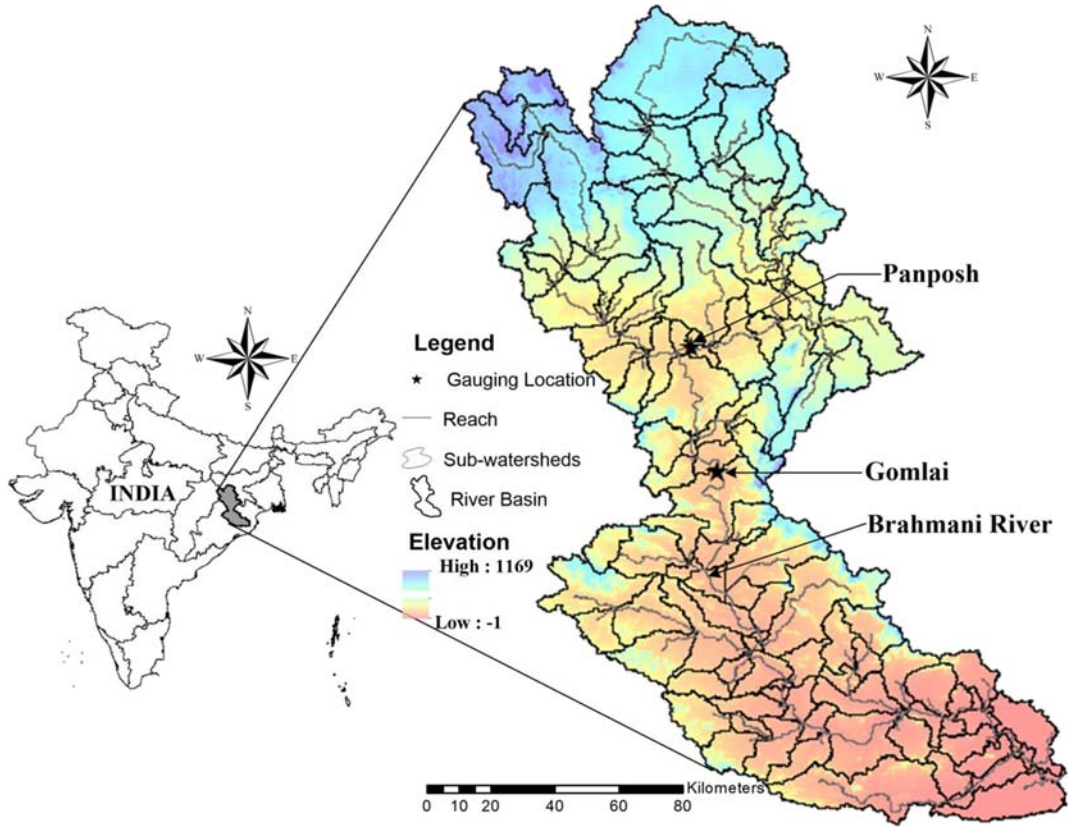

Fig. 1 Study area (Brahmani River basin) location

average annual soil loss in a region as estimated by RUSLE is represented as

$$SE = R \times K \times L \times S \times C \times P \quad (1)$$

where SE is the estimated potential soil loss (t ha^{-1} year^{-1}); R is the rainfall erosivity index (MJ mm ha^{-1} h^{-1} year^{-1}); K is the estimated soil erodibility factor (t h ha MJ^{-1} ha^{-1} mm^{-1}); LS is the topographic factor that combines the slope length and slope steepness factor; C is the land use specific cover management factor; P is the conservation support practice factor.

Further, a more detailed description about the steps followed to estimate the above-said *RUSLE* parameters are illustrated in Fig. 2.

Derivation of RUSLE parameters

Rainfall erosivity factor (R factor)

R factor corresponds to the potential capability of the rainfall intensity to result in soil erosion from an uncovered surface (Renard et al. 1997). Rainfall erosivity is the long term average value of the yearly rainfall erosivity value for a particular location. It solely depends on the physical characteristics of the rainfall, viz., the amount of rainfall, intensity of rainfall, raindrop size, terminal velocity, and kinetic energy. Wischmeier and Smith (1978) established an initial relationship between rainfall erosivity and rainfall depth and later revised by Arnoldus (1980) capable of capturing the monthly rainfall dynamics in a region, as given by

$$R = \sum_{i=1}^{12} 1.735 \times 10^{\left(1.5 \times \log\left(\frac{P_i^2}{P}\right) - 0.08188\right)} \quad (2)$$

where P_i is the monthly rainfall (mm) in the i^{th} month; P is the magnitude of average annual rainfall (mm). The climatic characteristics of the chosen study site resembles the climate, where the original Arnoldus equation was developed. To estimate the R factor, monthly time series of rainfall for the period 1951–2015 was used in this study. The estimated R factor identified the critical regions where the rainfall causes the maximum potential

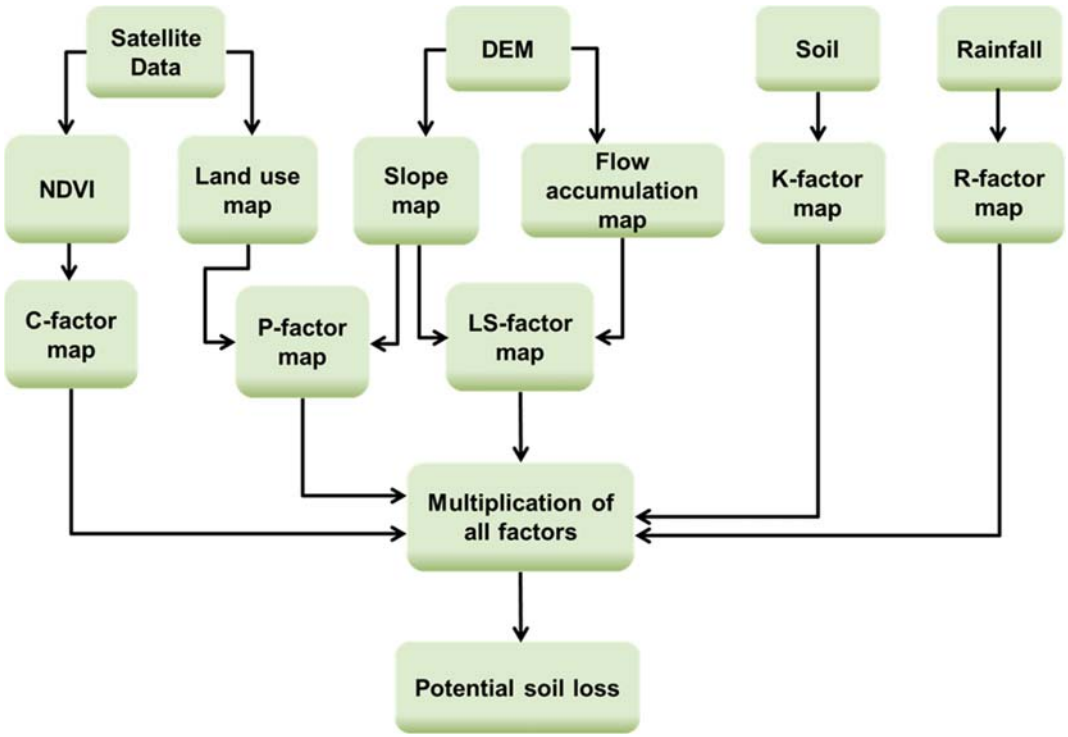

Fig. 2 Flow chart for the estimation of soil erosion using RUSLE

detachment of soil particles due to the caused rainfall intensity.

Soil erodibility factor (K factor)

The K factor is determined on the basis of physical and chemical properties of the top soil layer of a region. It measures the inherent erodibility potential of soil particles through detachment, and subsequent, transportation caused by the rainfall and generated streamflow. The K factor is prone to maximum variability in a locality while other factors remain unchanged (Wischmeier and Smith 1978). The K factor was computed using the previously defined soil texture estimates as given by Wischmeier and Smith 1978:

$$K = 0.1317 \times \frac{0.00021 \times M^{1.14} \times (12-a) + 3.25(b-2) + 2.5(c-3)}{100} \quad (3)$$

where M is a function of soil textural parameters, given by

$$M = (\%Silt + \%VFS) \times (100-\%Clay)$$

a is the soil organic matter in percentage; b is the soil structural code used in Eq. (3), viz., clay = 1, clay loam and silty clay loam = 2, loam and silty loam = 3; c is the permeability of soil profile (Vaezi et al. 2010) as classified based upon the saturated hydraulic conductivity (K_s) as presented in Table 1. The K factor value ranges from 0.023 to 0.039 t h ha MJ^{-1} ha^{-1} mm^{-1} in the present study, where lower value corresponds to soils with least susceptibility to erosion while higher value signifies to soils with higher susceptibility to erosion caused by rainfall and runoff.

Slope length factor (L factor)

The slope length is expressed as the linear distance between the overland flow origin point to the location where the slope extent reduces adequately to initiate deposition process. The erosive velocity gradually increases with increase in the slope length, and subsequently, intensifies the resulting surface runoff. Since field-scale measurement of L and S factor is highly cost and time expensive, indirect remote-sensing based approaches are getting significant attention for such estimation. Hence, the DEM-based approach suggested by Desmet and Govers (1996) in the USA condition, was applied to address the inherent limitations involved in the field-scale estimation of L factor, given as

$$L = \frac{\left(A_{ij-in} + D^2\right)^{m+1} - A_{ij-in}^{m+1}}{D^{m+2} \times X_{ij}^{m} \times 22.13^{m}} \quad (4)$$

where $L_{i,j}$ is the slope length factor with cell coordinates (i, j); $A_{i,j\text{-in}}$ is the contributing area at the inlet of the respective cell grid having coordinates (i, j) (m^2); m is the exponent of slope length factor used in the RUSLE.

Slope steepness factor (S factor)

The soil erosion potential of the concerned location is characterized by the S factor which gets substantially affected by the slope steepness. The slope steepness factor is elucidated as the ratio of soil loss from a field having certain slope gradient to that from an experimental plot having 9% slope under identical conditions. To calculate the S factor, the approach suggested by McCool et al. (1987) was adopted, as given by

$$S = 10.8\mathrm{Sin}\theta + 0.03 \quad if \quad (S < 9\%) \quad (5a)$$

$$S = 16.8\mathrm{Sin}\theta - 0.50 \quad if \quad (S \geq 9\%) \quad (5b)$$

where θ is the slope magnitude, represented in degree.

The L and S factors are combinely known as the topographic (LS) factor which represents the behavior of surface soil, and subsequently, influences the soil erosion processes. Precisely, the transportation phase of the soil erosion process is mostly governed by the topographic factor.

Crop cover management factor (C factor)

The C factor describes the consequences of crop growth and productivity, soil cover, subsurface bio-mass on the soil erosion process. It is represented as the ratio of soil loss in a cropped land under managed conditions to the respective loss from a continuous tilled, fallow land (Wischmeier and Smith 1978). The relationship proposed by Zhou et al. (2008) and Kouli et al. (2009) were adopted in this study to estimate the C factor, as given by

$$C = \exp\left(-\alpha \frac{NDVI}{\beta - NDVI}\right) \quad (6)$$

where α and β are the shape parameters that determine the shape of NDVI-C curve, wherein the values of α and β values were treated as 2 and 1, respectively (Van der Knijff et al. 2000). The spatial variation of C factor is shown in Fig. 4d which varies between 0.16 and 1.

Conservation practices factor (P factor)

The P factor is depicted by the loss of soil under a particular conservation practice to the respective soil loss from a field having continuous up- and downslope tillage (Renard et al. 1997). The values of P factor were selected on the basis of the magnitude of slope and followed soil management practices in a region. The previously land use map of the study area was overlaid in conjunction with the information obtained regarding the management practices adopted in this area, and subsequently, the value of P factor was obtained. Different weights were assigned to individual management practices and land slope classes for the analysis. The management practices which reduce the soil erosion to a greater extent were assigned higher weights and vice versa. Later on, a subsequent raster overlay operation was performed in ArcGIS 10.1 for developing the P factor map. The value of P factor ranges from 0 to 1, where the values close to 1 correspond to the critical erosion-prone areas. The P factor value adopted for different combinations of land slope and management practices are depicted in Table 2.

Table 1 Adopted profile permeability value (c) classification

c value	K (mm h^{-1})
1	> 150
2	50–150
3	15–50
4	5–15
5	1–5
6	< 1

Estimation of sediment yield and soil erosion potential

Once the various RUSLE parameters computation is over, the thematic layers of individual RUSLE parameters were prepared using the ArcGIS 10.1 software. All the prepared thematic layers were then multiplied using raster calculator tool of the ArcGIS 10.1 software. This process generates a spatially distributed soil erosion map of the concerned basin. However, from management prospective, sediment yield (SY) has more importance

over the potential soil erosion as they quantify the amount of soil moving out from the watershed. Hence, a sediment delivery ratio (SDR) based sediment yield estimation approach has been incorporated in this study. Sediment yield is the amount of total erosion taking place in the catchment that was not accumulated before and going out from the watershed in a given time span. In general, sediment yield at a point location is a function of the total erosion and SDR magnitude at that point. The fraction of the total erosion that is getting transported to the measurement location is termed as SDR, which signifies the sediment transport efficiency of the concerned location. The SDR estimation approach suggested by USDA SCS is adopted in this study, given by

$$SDR = 0.51 \times A^{-0.11} \tag{7a}$$

$$SY = SDR \times SE \tag{7b}$$

where A is the watershed area in km^2; and SY is the sediment yield (t ha^{-1} year^{-1}).

The sediment yield so estimated here corresponds to the actual soil loss taking place in the concerned location and estimated for individual image pixels having a spatial resolution of 30 m. In order to identify the critical locations for implementing the best management practices (BMPs), a systematic categorization of potential soil erosion location is of utmost importance. Hence, a user-defined classification system has been introduced in this study which consists of six potential soil erosion zones based on the user-defined individual soil erosion threshold value as depicted in Table 3. Further, the similar classification criteria were well extended to understand the sediment yield dynamics over the catchment of BRB.

Table 2 *P*-factor values for different slope and land management classes

Slope (%)	**Land management practices**	*P* factor
0.0–7.0	Strip cropping	0.55
7.0–11.3	Contour bund	0.60
11.3–17.6	Graded bund	0.80
17.6–26.8	Broad-base terrace	0.90
> 26.8	Bench terrace	1.00

Climate change impact assessment

The climatic of the study area is subjected significant alteration in the future time scales. In the climate change context, the RUSLE-based soil erosion process is subjected to variation due to changes in the future rainfall pattern, LULC, and followed management practice. However, the estimation of future LULC change and possible addition of management practice is beyond the scope of this study. Moreover, the topographic factor which is primarily a function of soil type and texture is subjected to a very slow change in the future time scales, hence, were assumed constant in this study. The variation in the rainfall magnitude and intensity directly affects the R factor of the RUSLE model. Hence, to predict the soil erosion potential of study area under climate change scenario, the revised estimation of R factor is inevitable.

As precipitation is the only desired climatic variable that is prone to alteration in its magnitude in the future climate change context, emphasis was given to analyze the future precipitation anomalies in the BRB. Recently, many general circulation model (GCM) and regional climate model (RCM) are widely used across the globe to quantify the future climatic alterations ranging from field scale to regional scale applications (Padhiary et al. 2019; Dash et al. 2020b). The Hadley Center Global Environmental Model, Version 2, Earth System (HadGEM2-ES) which is available at a spatial resolution of 1.875° × 1.25° was used in this study. Prior to the analysis of soil erosion potential of individual sub-basins, the GCM was bias corrected using the quantile mapping bias-correction technique, and subsequently, downscaled to a spatial resolution of 1 km × 1 km. A 5th order polynomial is fitted to each pixel in the GCM

Table 3 User-defined classification to identify potential soil erosion zones

Serial no.	Soil erosion zone	Potential soil loss/sediment yield value (t ha^{-1} year^{-1})
1	Very low	0–5
2	Low	5–10
3	Moderate	10–20
4	High	20–40
5	Very high	40–80
6	Extreme	> 80

output to obtain the time trend and a cubic convolution approach of interpolation approach was followed to downscale it to 1 km spatial resolution. The recalculated difference was added to the baseline to obtain the downscaled rainfall value. The rainfall data was analyzed for the four representative concentration pathways (RCPs), i.e., 2.6, 4.5, 6.0, and 8.5 for four future time slices of 2030, 2050, 2070, and 2080. The centroid point of individual sub-basin of the BRB was determined using the ArcGIS 10.1 software and respective precipitation values were extracted for all the RCP scenarios. Further, using the methodology discussed in "Rain erosivity factor (*R* factor)" section, modified *R* factor map was prepared for all the individual RCP scenarios using the downscaled precipitation estimates. Further, this *R* factor value was multiplied with the *K*, *L*, *S*, *C*, and *P* factor, in order to generate the potential soil erosion maps for future climate change scenarios. Similarly, these estimated soil erosion values were multiplied with the previously generated SDR map to obtain the sediment yield across all the pixel locations. Finally, the percentage change in the sediment yield between future projection and baseline period was calculated for individual sub-basins of the BRB followed by identification of critical erosion-prone locations of the BRB.

Results and discussions

The monthly average rainfall values of 23 IMD grid points for the year 1951–2014 were used in this study for the estimation of *R* factor in individual grid cells of BRB. The spatial variation between the rainfall depth and erosivity across these selected locations is presented in Fig. 3. For most of the locations, the rainfall erosivity value bears a direct linear relationship with the rainfall depth magnitude, the highest being observed at grid#222. Using the point rainfall erosivity values, inverse distance weighting (IDW) approach of interpolation had been incorporated to prepare spatial distribution map of *R* factor and presented in Fig. 4a. The rainfall erosivity value was found to be ranging between 1937 and 4867 MJ mm ha^{-1} h^{-1} $year^{-1}$ and majority of the values were below 2500 MJ mm ha^{-1} h^{-1} $year^{-1}$. The higher numbers of such values were confined to the central part of the basin and could be consequenced due to the erratic distribution of rainfall events over the study basin.

The *K* factor thematic layer was prepared by adopting the previously discussed methodology (the "Soil erodibility factor (*K* factor)" section) and spatial distribution of *K* factor values presented in Fig. 4b. The mean of *K* factor was observed to be 0.031 t h ha MJ^{-1} ha^{-1} mm^{-1} with the higher values were distributed in the downstream regions of the BRB. Since finer resolution soil parameters were used in this case, standard deviation value of 0.003 t h ha MJ^{-1} ha^{-1} mm^{-1} was observed among the spatially distributed value of the *K* factor. It was found that for loam soil, the *K* factor was highest, i.e., 0.03946 t h ha MJ^{-1} ha^{-1} mm^{-1} and was more prone to the soil erosion hazard.

Both the *L* and *S* factors were calculated individually and later combined as the topographic factor (*LS* factor) which was calculated through multiplication of the *L* and *S* factor. A spatially distributed thematic layer of *LS* factor was generated for this study basin and was illustrated in Fig. 4c. The value of *LS* factor was found to be varying between 0.03 for flat regions to 74 in case of steep slopes. More than 80% of catchment area was covered by *LS* factor value between 1 and 5, indicates less diverse topography of the basin. Moreover, all the pre-defined ranges of *LS* factor were found to be uniformly distributed and indicated the presence of a moderately low to moderately high *LS* factor value in the study region. Thus, the least effect of topography over the soil erosion process was observed throughout the soil erosion modeling of the BRB.

The NRSC procured LULC map at a spatial scale of 1:250000 was considered as the reference map for performing the supervised land use classification. Sixteen distinct land-use types were identified from the resulting classification, given by (1) residential-high density urban area, (2) fallow land, (3) water bodies, (4) evergreen forest, (5) deciduous forest, (6) kharif crop, (7) zaid crop, (8) rabi crop, (9) double and triple crop, (10) shrub land, (11) grass land, (12) barren or sparsely vegetated land, (13) gullied land, (14) scrub land, 15) orchard, and (16) shifting cultivation and shown in Fig. 5a. The NDVI map was generated using the Landsat TM 8 (OLI) image followed by the creation of *C* factor thematic layer map. During the course of computation of *C* factor, the parameters α and β were considered as 2 and 1, respectively, as obtained from the study conducted by Van der Knijff et al. (2000). These adopted parameters justified the exponential relationship among the NDVI and *C* factor. The pixel wise NDVI values were overlain to the basin LULC map

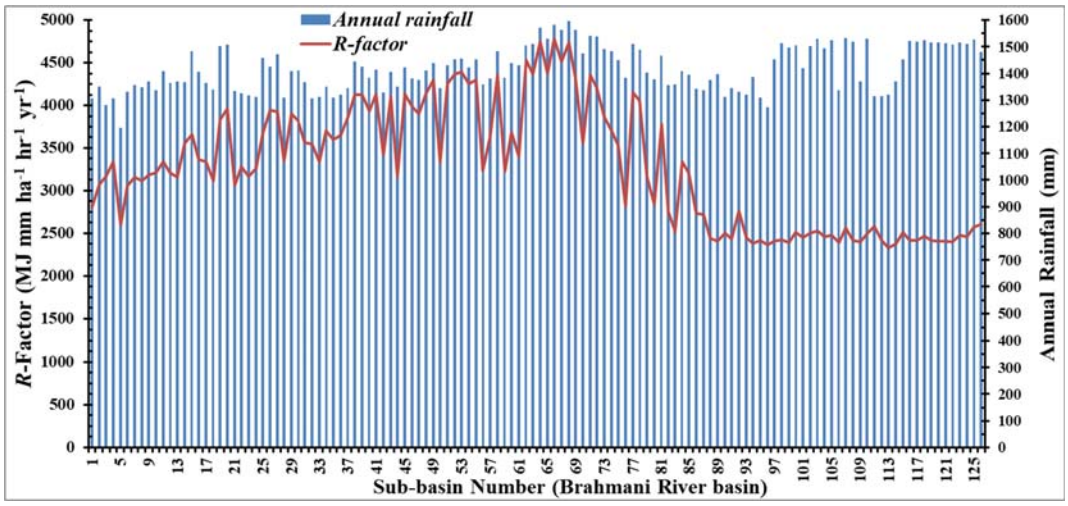

Fig. 3 Spatial variation of rainfall and erosivity in Brahmani River basin

(raster map) to construct a spatially distributed *C* factor map of the basin. For the crop lands and gullied lands, the effect of crop types and management practices adopted for reclamation of gullied land were conceptualized to generate a realistic *C* factor map. The *C* factor ranged from 0.16 to 1, wherein the lower values corresponded to dense evergreen forest regions and higher values signified to bare rocky terrains (Fig. 4d).

The *P* factor corresponds to the reduced soil erosion hazard as a result of the protective management operations/structures adopted in a specific region. Hence, in this study, an integrated land slope and management operation based *P* factors were generated and presented in Table 2. Incorporating these values in raster calculator and by providing suitable query, a spatial map of the *P* factor for the whole basin was prepared (Fig. 5b). The *P* factor value was found to be ranged from 0 to 1, wherein 0 indicates areas having the lowest erosion potential as a consequence of suitable adaptive measures and 1 corresponds to the severe erosion-prone areas consequenced due to lack of suitable management practices.

Estimation of annual potential soil loss and sediment yield

To estimate the average annual potential soil loss, all the six erosion causing factors so prepared in the form of raster maps were multiplied in ArcMap 10.1 with use of the raster calculator tool. In Fig. 5c, the annual potential soil loss for the whole basin represented in the form of a spatial plot depicting the pixel-wise variation in the soil erosion across the BRB. Further, by adopting the user-defined classification criteria, the area under potential soil loss and sediment yield for individual classes were presented in Table 4. The reclassified soil erosion map revealed that very high and extreme soil erosion-prone areas were the two dominant erosion classes present in the basin, whereas the area under low erosion class was very less. Lower and upper part of the basin was shrouded with less soil erosion potential, approximately 0 to 5 and 5 to 10 t ha^{-1} $year^{-1}$. This kind of soil erosion distribution may be due to the presence of the plain topography and lower rainfall erosivity value over these locations. The default erosion potential value of waterbodies was treated as zero and can be well inferred from the Fig. 5c. The major portion of the BRB, i.e., 54.20% was under the extreme soil erosion risk class and 33.19% under very high soil erosion risk class, located mostly toward the ridge line and central part of the basin. The remaining soil erosion risk classes, such as high, moderate, and very low account for 9.27%, 0.72%, and 2.31% of total basin area, respectively.

The SDRs values were obtained using USDA SCS formula, for all the 126 sub-basins of the area. The SDR values were found to vary from 0.22 to 0.54 and distributed in an un-even manner in the basin (Fig. 5d). A SDR value of 0.22 to 0.32 was covering more than 95% of the whole basin. The minimum basin area was found to be falling under the SDR range of 0.32 to 0.42. These estimated values of SDR were used in the equation suggested by Wischmeier and Smith 1978, and the sediment yield (*SY*) was considered for individual sub-

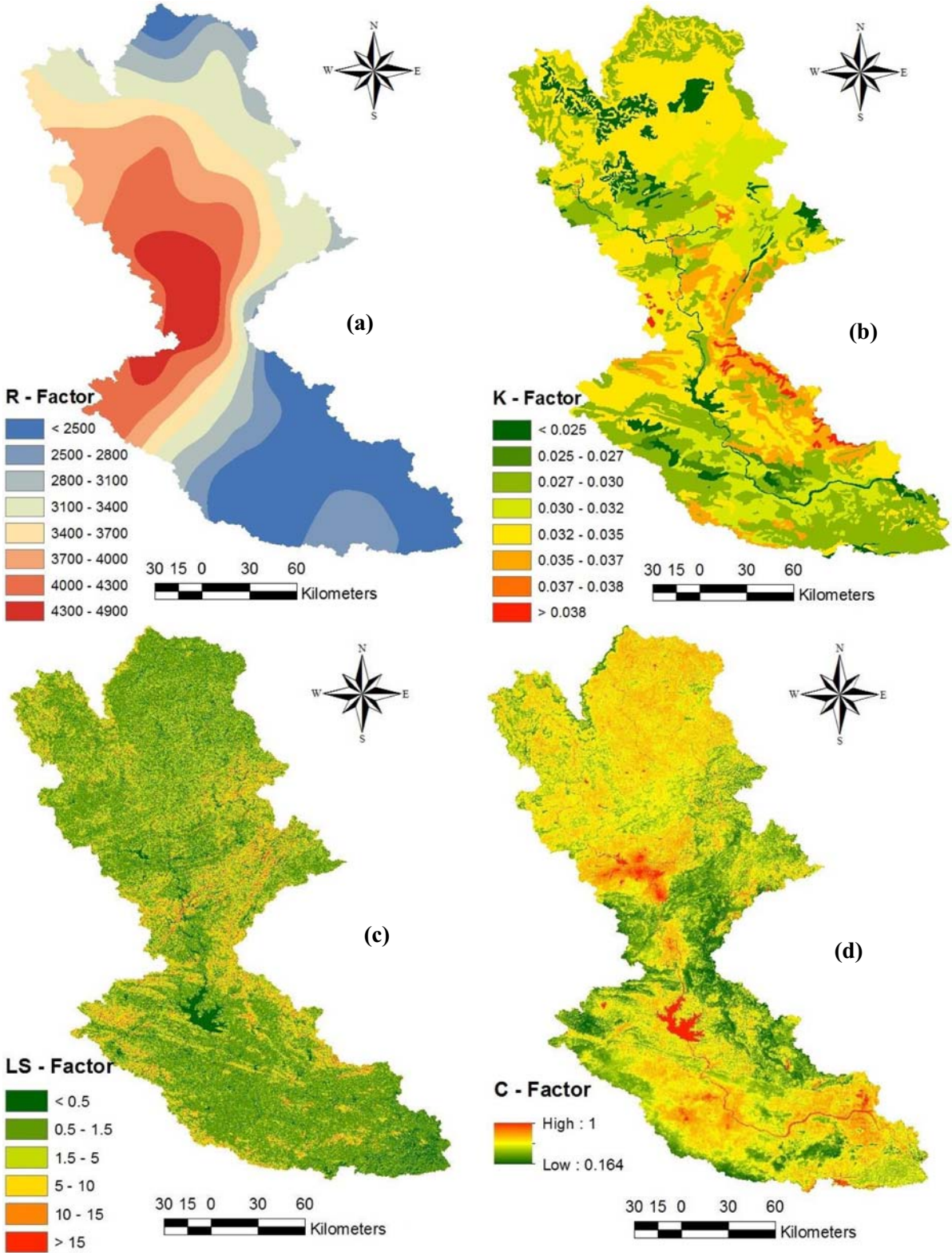

Fig. 4 The thematic layer represent (**a**) rainfall erosivity factor map; (**b**) soil erodibility factor map; (**c**) topographic factor map; and (**d**) cover management factor map of the study area

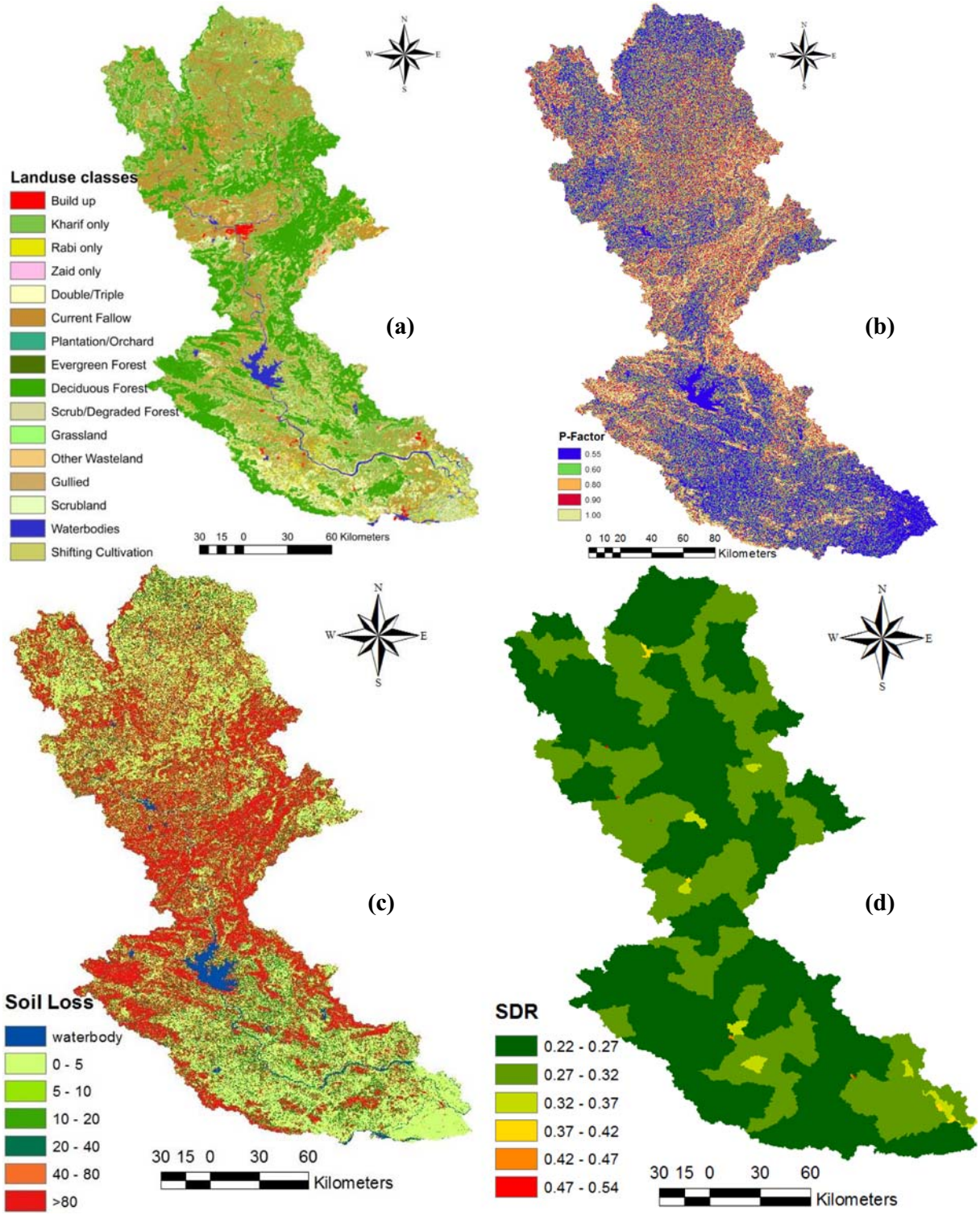

Fig. 5 (**a**) Land use map; (**b**) conservation practice factors map; (**c**) annual potential soil loss map; and (**d**) sediment delivery ratio map of the Brahmani River basin

Table 4 Categorization of the soil erosion potential and sediment yield

Erosion class	Erosion potential	Potential soil loss area		Sediment yield area	
		(km^2)	(%)	(km^2)	(%)
1	Very low	917.03	2.31	1188.30	2.99
2	Low	110.97	0.28	2738.25	6.90
3	Moderate	286.85	0.72	13,985.10	35.28
4	High	3677.27	9.27	14,195.46	35.81
5	Very high	13,154.22	33.19	7674.02	19.36
6	Extreme	21,484.57	54.20	42.14	0.10

basins of the case study. The *SY* values in the basins were found to be varying between 0.96 and 133.31 t ha^{-1} $year^{-1}$ for the concerned study period. For classifying the critical sediment yield regions, the estimated *SY* values were categorized to six classes, i.e., 0-5, 5-10, 10-20, 20-40, 40-80, and > 80 t ha^{-1} $year^{-1}$ and the reclassified map is illustrated in Fig. 6. The *SY* values in the ranges of 20 to 40 (high soil erosion potential), 10 to 20 (moderate soil erosion potential), and 40 to 80 (very high soil erosion potential) t ha^{-1} $year^{-1}$ covered

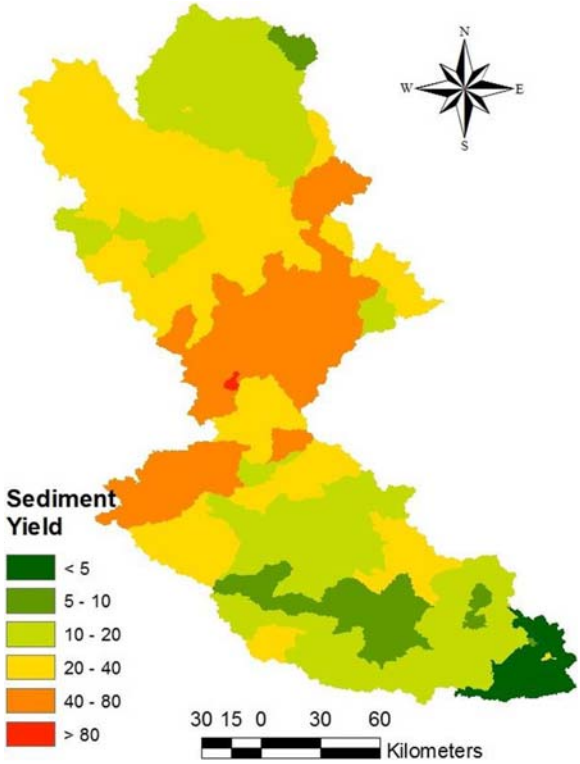

Fig. 6 Sediment yield map of the study basin

35.81%, 35.28%, and 19.36% of the total basin, respectively. The area under remaining soil erosion risk classes like very low, low, and extreme were found to be very less in the BRB. The areas having soil loss ranging between 10 and 20 t ha^{-1} $year^{-1}$ were mostly flat areas with evergreen forest cover (Fig. 7a). Similarly, areas having soil erosion ranging from 20 to 40 t ha^{-1} $year^{-1}$ were typically from the agricultural lands, residential areas, while some were under the deciduous forest areas having smaller slope ranges (Fig. 7b) having the similar soil erosion potential in most of the areas of the watershed. In past, areas near Dholduba, Kindhal, Remal dam in the Dandadhar reservoir of Odisha had experienced similar severity of soil erosion. Further, areas with potential soil loss in the range of 40 to 80 t $ha^{-}1$ $year^{-1}$ were generally agricultural and deciduous forested lands with higher slopes (Fig. 7c) and found near the Birkera, Badbhulta locations of Odisha and Hatnabera and Sindribera locations of Jharkhand state falls under this class of soil loss potential. Areas with potential soil loss > 80 t ha^{-1} $year^{-1}$ were mostly experienced in steeper slope, riverbank areas, urban areas, deciduous forest, and scrub lands (Fig. 7d). These soil erosion-prone areas were confined to the Ludhuni and Bartengada locations of Odisha. For those areas, the river followed a meandered path, which could be the prime cause behind this higher magnitude of soil erosion potential. Moreover, the presence of industrial plants in these locations could have accelerated the soil erosion process to a greater extent. The higher *SY* values were mostly observed at the central part of the study basin, which was an indicative of the fact that a higher *LS* factor in conjunction with an increased *R* factor value has consequenced this hazard.

Estimation of *R* factor map in a climate change context

In the present study, the impact analysis was limited to the effect of climate change only. It was assumed that no change will happen to the LULC and topography of the area during the concerned period. Thus, only *R* factor of RUSLE is susceptible to alteration in a climate change scenario due to the variation caused to the rainfall magnitude and intensity of the location. Therefore, before analyzing the changes that happened to the soil erosion potential over a locality, it was quite imperative to analyze the spatiotemporal variation in *R* factor across the concerned region under the climate change context. The future *R* factor maps for all the four scenarios and

Fig. 7 (**a**) Areas with soil loss between 10 and 20 t ha^{-1} year^{-1}; (**b**) 20 and 40 t ha^{-1} year^{-1}; (**c**) 40 and 80 t ha^{-1} year^{-1}; and (**d**) more than 80 t ha^{-1} year^{-1}

for all the time slices were generated and shown in Fig. 8.

Climate change impact analysis on future potential soil erosion

The *R* factor maps prepared for each scale of time and for individual RCPs were multiplied with the previously estimated soil erodibility factor (*K*), topographic factor (*LS*), cover management factor (*C*), and conservation practice factor (*P*) to get the potential soil loss in each time scale of individual RCPs. Then the SDR value for each sub-basin was multiplied with each potential soil loss value of each time scale to get the sediment yield value of each time period of individual RCPs. Further, the percentage change in SY with reference to the base period was calculated. Later on, a spatial sediment yield map showing percentage change with respect to the base period was generated by averaging over all time scales and presented in Fig. 9. The minimum, maximum, and average values of percentage change in sediment yield were calculated and a graphical representation was illustrated in Fig. 10.

From the general comparison between the base period soil erosion and the future soil erosion, it was evident that erosion rates were significantly higher in the future time scales as the rainfall depth was higher in the future time slices. Moreover, the spatial distribution of the soil erosion process was highly discrete and uncertain in the future time period. The future climate change scenario also signified a gradual growth of soil erosion process across a significant portion of the BRB. However, the rate of growth was found to be highly un-even across the complete spatial domain of the basin. Only, 9.5% of complete basin area will experience more than 100% change in sediment yield and such areas were certainly confined to the localities of the river and reservoir banks. Upon an increase in the rainfall magnitude, the

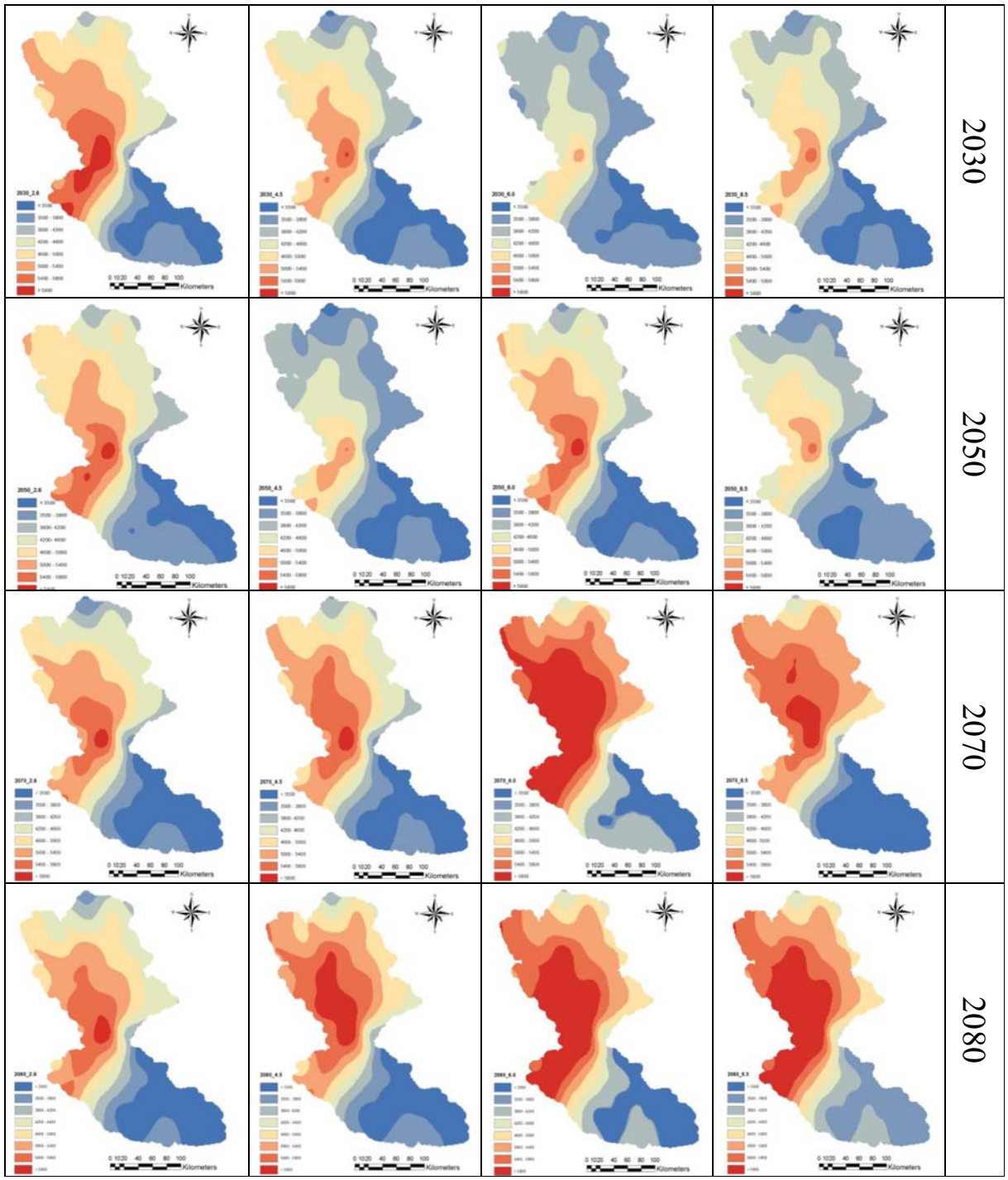

Fig. 8 Variation in *R* factor over all future time slices

erosion rate will increase, and subsequently, will cause more damage to the soil resource of that location. A detailed analysis revealed that only 4.8% of the total basin area may experience a change between 75 and 100% for sediment yield. Similarly, the areas adjacent to the tributaries of Brahmani River will be at higher risk of erosion due to increased streamflow of the river as confirmed by the study conducted by Dash et al.

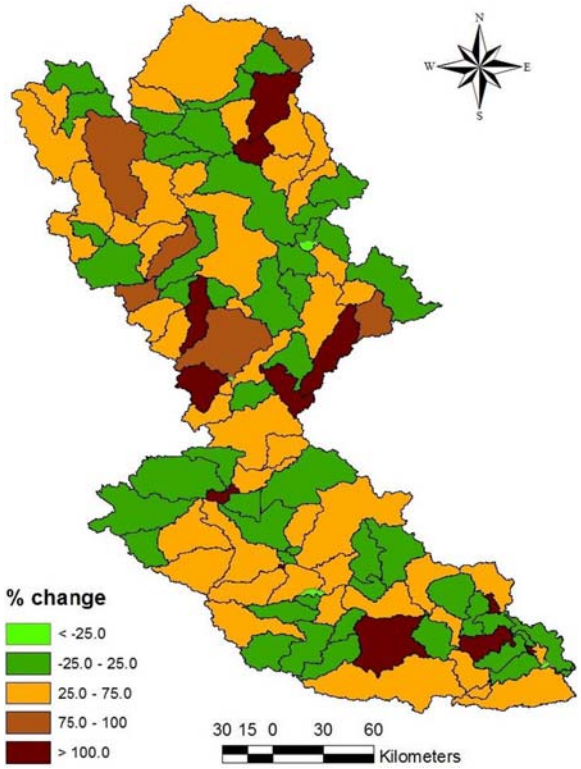

Fig. 9 Percentage change in sediment yield averaged over all RCPs of all time scale

(2020b). Further, 36.5% of the basin area showed the increase in sediment yield between 25 and 75% signifying moderate erosion hazard in the BRB in future time scales. As predicted earlier, climate change tends to increase the spatial variability as well as the magnitude of the rainfall, and becomes the key reason behind the increase in soil erosion potential in the study locations. The higher percentage of area, i.e., 42.9% showed variation in percent change between −25 and 25%, which were an indicative of the fact that deposition and erosion rate in those areas will be in the same rate and will be treated as stable locations from the perspective of erosion hazard. This indicated the fact that climate change impact would be considerable in the majority of the sub-basins of BRB. Therefore, the above-said locations would be at less risk of erosion. Similarly, 6% of the basin area showed a percentage change in SY as less than 25% corresponds to minimal attention of policymakers in the future. That location where percentage decrease showed maximum was verified to be well covered with vegetation and less severe slope classes. The base period sediment yield in those areas was also found to be less and treated as very low erosion-prone regions. Figure 10 shows the graphical representation of the sub-basin-wise minimum, average, and maximum change in sediment yield and it can be inferred that the sub-basin 73 will have the maximum percentage change in SY. As this area mainly covers the deciduous forest and fallow lands, the SY in the base year was also high in this sub-basin. Moreover, in the future time period, those areas may experience higher soil erosion threats.

Conclusions

The objective of the study was to assess the soil erosion risk in the present and future time period in the BRB that covers major portions of the states like Odisha,

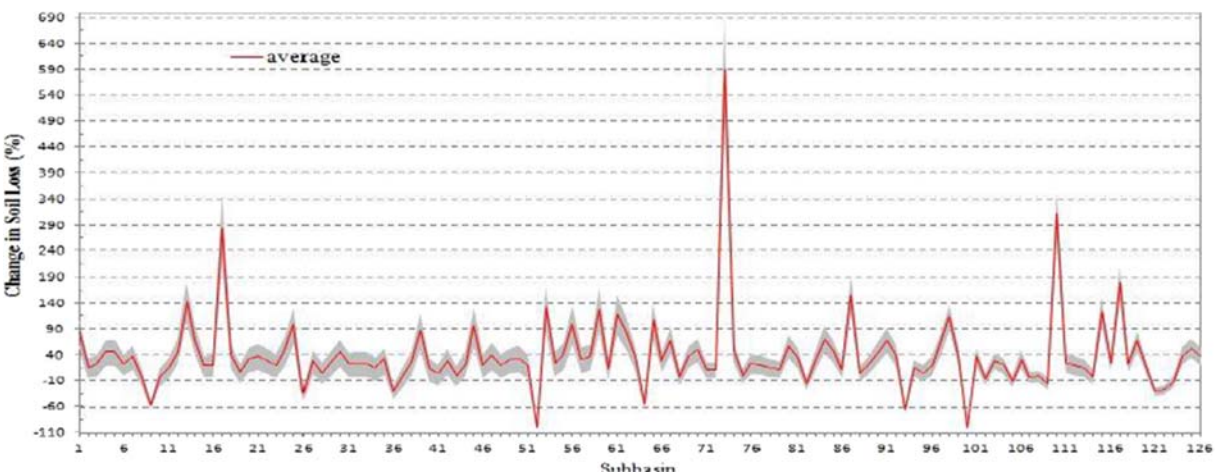

Fig. 10 Graphical representation of percent change in sediment yield with minimum, average, and maximum range value

Jharkhand, and Chhattisgarh and frequently experiencing the adverse climatic change conditions such as droughts, floods, and tropical cyclones in the recent whiles. In this study, the RUSLE model along in conjunction with the remote sensing and GIS technique was used to analyze the potential soil erosion and SY of the BRB. Due to the unavailability of necessary observed data, partial features were derived from the satellite imageries with suitable pre- and post-processing operations. By overlying the five essential thematic layers, the potential soil erosion map for the basin was generated. Further, implementing a novel methodology, the SDR map was derived, and subsequently, used to estimate the SY occurring from individual sub-basins. Climate change impact analysis was carried out for the future time scales of 2030, 2050, 2070, and 2080. It was presumed that in the upcoming years, only the rainfall erosivity factor will vary because of the variation in rainfall depth and intensity while all other factors such as LULC and topography will remain the same as that of the base period. The *R* factor maps for all the future time periods under all RCPs scenarios were prepared as per the predicted rainfall from HadGEM2-ES GCM model. These newly generated *R* factor maps were then used to obtain the sediment yield fluxes for the future periods and subsequently, the percentage change in SY with reference to the base year was derived for all time period of all RCPs. Some critical observations pertaining to this research are depicted below.

i) The potential soil loss in the BRB varies between 5 and 319.55 t ha^{-1} $year^{-1}$, wherein 54.2% of basin area have a rate of soil loss more than 80 t ha^{-1} $year^{-1}$.
ii) The SDR value of the area lies in the range of 0.22 to 0.54 resulting in SY of the basin to vary in the range of 0.96 to 133.31 t ha^{-1} $year^{-1}$. The SY estimated by using the developed SDR map indicates that most of the basin area (35.81%) has SY value lies between 20 and 40 t ha^{-1} $year^{-1}$.
iii) The critical areas from both potential soil erosion and SY perspective are confined to the central part of the basin due to the presence of more tributary rivers and industries.
iv) In the climate change context, 42.9% of the area (maximum) shows percent change in sediment yield between −25 and 25% and signifying minimal alteration to the sediment yield value. However, 9.5% of basin area experienced a change more than 100% and are mostly confined to the central part where the Rengali reservoir is located. This envisages, the condition of critical areas from sediment yield perspective is going to be worsen in the future.
v) The sub-basin 73, which is situated just downstream of the Rengali reservoir, was found to be the most critical sub-basin from erosion point of view, thereby warrants critical consideration from the policymakers.

The outcomes of this study indicate that the GIS-based RUSLE approach can be applied for quantification of soil erosion potential across BRB during both present and future climate scenarios. Moreover, the identified critical locations and expected change in soil erosion potential value may help the policymakers by giving an insight about the locations, where the soil conservation structures can be constructed, so that the soil erosion can be checked within the accepted limit. Conclusively, the methodology proposed herein can be well extended to any global river basins for catchment-scale assessment of soil erosion hazard.

Acknowledgments The authors are thankful to the NICRA project at ICAR-IISWC Dehradun for partially funding the present research. Thanks are extended to Ms. Monika Rawat for assisting in the future climate data preparation. The fellowship received by the first author from the TEQIP program is duly acknowledged.

Compliance with ethical standards

Conflict of interest The authors declare that they have no conflict(s) of interest.

References

Adhikary, P. P., Sena, D. R., Dash, C. J., Mandal, U., Nanda, S., Madhu, M., Sahoo, D. C., & Mishra, P. K. (2019). Effect of calibration and validation decisions on streamflow modeling for a heterogeneous and low runoff–producing river basin in India. *Journal of Hydrologic Engineering 24*(7), 05019015(1–12).

Alatorre, L. C., Begueria, S., & Garcia-Ruiz, J. M. (2010). Regional scale modelling of hillslope sediment delivery: A case study in the Barasona reservoir watershed (Spain) using WATEM/SEDEM. *J Hydrol, 391*(1–2), 109–123.

Arnáez, J., Lana-Renault, N., Lasanta, T., Ruiz-Flaño, P., & Castroviejo, J. (2015). Effects of farm-ing terraces on hydrological and geomorphological processes. *Catena., 128*, 122–134.

Arnoldus, H. M. J. (1980). An approximation to the rainfall factor in the universal soil loss equation. *Assess Erosion*, 127–132.

Biswas, S. S., & Pani, P. (2015). Estimation of soil erosion using RUSLE and GIS techniques: A case study of Barakar River basin, Jharkhand, India. *Model Earth Syst Environ, 1*, 42.

Boomer, K. B., Weller, D. E., & Jordan, T. E. (2008). Empirical models based on the universal soil loss equation fail to predict sediment discharges from Chesapeake Bay catchments. *J Environ Qual, 37*, 79–89.

Chandramohan, T., Venkatesh, B., & Balchand, A. N. (2015). Evaluation of three soil erosion models for small watersheds. *Aquatic Procedia, 4*, 1227–1234.

Chen, T., Niu, R., Li, P., Zhang, L., & Du, B. (2011). Regional soil erosion risk mapping using RUSLE, GIS, and remote sensing: A case study in Miyun watershed, North China. *Environ Earth Sci, 63*, 533–541.

Dash, S. S., Sahoo, B., & Raghuwanshi, N. S. (2019). A SWAT-copula based approach for monitoring and assessment of drought propagation in an irrigation command. *Ecol Eng, 127*, 417–430.

Dash SS, Sahoo B, Raghuwanshi NS (2020a). A novel embedded pothole module for soil and water assessment tool (SWAT) improving streamflow estimation in paddy-dominated catchments. J Hydrol, 125103.

Dash, S. S., Sena, D. R., Mandal, U., Kumar, A., Kumar, G., Mishra, P. K., & Rawat, M. (2020b). A hydrological modelling-based approach for vulnerable area identification under changing climate scenarios. *J Water Clim Change*. https://doi.org/10.2166/wcc.2020.202.

Desmet, P. J. J., & Govers, G. (1996). A GIS procedure for automatically calculating the USLE LS factor on topographically complex landscape units. *J Soil Water Conserv, 51*(5), 427–433.

Gabriels, D., & Cornelis, W. M. (2009). Human-induced land degradation. *Land Use Land Cover Soil Sci, 3*, 131–143.

Intergovernmental Panel on Climate Change Fourth Assessment Report, Climate change (2007): Synthesis report. 1–76.

Kouli, M., Soupios, P., & Vallianatos, F. (2009). Soil erosion prediction using the revised universal soil loss equation (RUSLE) in a GIS framework, Chania, Northwestern Crete. *Greece Environ Geol, 57*, 483–497.

Mahala, A. (2018). Soil erosion estimation using RUSLE and GIS techniques—A study of a plateau fringe region of tropical environment. *Arab J Geosci, 11*, 335.

McCool, D. K., Brown, L. C., Foster, G. R., Mutchler, C. K., & Meyer, L. D. (1987). Revised slope length factor for the universal soil loss equation. *Transactions of the ASAE, 30*(5), 1387–1396.

Nearing, M. A., Jetten, V., Baffaut, C., Cerdan, O., Couturier, A., Hernandez, M., Le Bissonnais, Y., Nichols, M. H., Nunes, J. P., Renschler, C. S., Souche're, V., & Van Oost, K. (2005). Modeling response of soil erosion and runoff to changes in precipitation and cover. *Catena., 61*, 131–154.

Ostovari, Y., Ghorbani-Dashtaki, S., Bahrami, H. A., Naderi, M., & Dematte, J. A. M. (2017). Soil loss estimation using RUSLE model, GIS and remote sensing techniques: A case study from the Dembecha watershed, Northeastern Ehiopia. *Geoderma Regional, 11*, 28–36.

Padhiary, J., Patra, K. C., Dash, S. S., & Uday Kumar, A. (2019). Climate change impact assessment on hydrological fluxes based on ensemble GCM outputs: A case study in eastern Indian River Basin. *J Water Clim Change*. https://doi.org/10.2166/wcc.2019.080.

Rawat, K. S., Mishra, A. K., & Bhattacharyya, R. (2016). Soil erosion risk assessment and spatial mapping using LANDSAT-7 ETM+, RUSLE, and GIS—A case study. *Arab J Geosci, 9*, 288.

Renard, K. G., Foster, G. A., Weesies, G. A., & McCool, D. K. (1997). Predicting soil erosion by water: A guide to conservation planning with RUSLE. In *USDA* (p. 703). Washington: Agriculture Handbook.

Vaezi, A. R., Bahrami, H., Sadeghi, S. H., & Mahdian, M. (2010). Spatial variability of soil erodibility factor (K) of the USLE in North West of Iran. *J Agric Sci Technol, 12*(2), 241–252.

Van der Knijff, J. M., Jones, R. J. A., & Montanarella, L. (2000). Soil erosion risk assessment in Europe. *Eur Soil Bureau*, 1–32.

Williams, J. R., & Berndt, H. D. (1977). Sediment yield prediction based on watershed hydrology. *Trans Am Soc Agric Biol Eng, 20*(6), 1100–1104.

Wischmeier, W. H., & Smith, D. D. (1965). Prediction rainfall Erosion losses from cropland east of the rocky mountains: A guide for selection of practices for soil and water conservation. *Agric Handb, 282*, 47.

Wischmeier W.H., Smith D.D., (1978). Predicting rainfall erosion losses: A guide to conservation planning. U.S. Dep. Agric., Agric. Handb. 537. Washington.

Zhou, P., Luukkanen, O., Tokola, T., & Nieminen, J. (2008). Effect of vegetation cover on soil erosion in a mountainous watershed. *Catena., 75*(3), 319–325.